Understanding the Mechanism of β-Hairpin Folding via ϕ-Value Analysis[†]

Deguo Du, Matthew J. Tucker, and Feng Gai*

Department of Chemistry, University of Pennsylvania, Philadelphia, Pennsylvania 19104

Received October 7, 2005; Revised Manuscript Received January 10, 2006

ABSTRACT: The folding kinetics of a 16-residue β-hairpin (trpzip4) and five mutants were studied by a laser-induced temperature-jump infrared method. Our results indicate that mutations which affect the strength of the hydrophobic cluster lead to a decrease in the thermal stability of the β-hairpin, as a result of increased unfolding rates. For example, the W45Y mutant has a ϕ-value of approximately zero, implying a folding transition state in which the native contacts involving Trp45 are not yet formed. On the other hand, mutations in the turn or loop region mostly affect the folding rate. In particular, replacing Asp46 with Ala leads to a decrease in the folding rate by roughly 9 times. Accordingly, the ϕ-value for D46A is determined to be ~0.77, suggesting that this residue plays a key role in stabilizing the folding transition state. This is most likely due to the fact that the main chain and side chain of Asp46 form a characteristic hydrogen bond network with other residues in the turn region. Taken together, these results support the folding mechanism we proposed before, which suggests that the turn formation is the rate-limiting step in β-hairpin folding and, consequently, a stronger turn-promoting sequence increases the stability of a β-hairpin primarily by increasing its folding rate, whereas a stronger hydrophobic cluster increases the stability of a β-hairpin primarily by decreasing its unfolding rate. In addition, we have examined the compactness of the thermally denatured and urea-denatured states of another 16-residue β-hairpin, using the method of fluorescence resonance energy transfer. Our results show that the thermally denatured state of this β-hairpin is significantly more compact than the urea-denatured state, suggesting that the very first step in β-hairpin folding, when initiated from an extended conformation, probably corresponds to a process of hydrophobic collapse.

The β-hairpin structural motif is proving to be very useful for understanding the thermodynamics and kinetics of β-sheet formation (*1*−*4*). Because of their structural simplicity, β-hairpins offer several advantages over β-sheet proteins in the study of how β-sheets fold and what determines their conformational stability. While most β-hairpins are small, some of them show cooperative folding behaviors that are characteristic of proteins. Therefore, the mechanism of β-hairpin folding has been a subject of great interest in recent years (*5*−*21*). While extensive equilibrium studies have yielded significant insights into our understanding of the molecular interactions that govern the thermodynamics of β-hairpin formation (*1*−*4*, *22*−*26*), the exact nature of how these interactions control the folding dynamics of β-hairpins is not well understood. For instance, the stabilizing effects provided by an appropriate turn sequence and a cluster of hydrophobic side chains have been shown to be essential for the stability of the β-hairpin fold (*2*, *23*−*26*). However, it is only recently that experimental studies have begun to explore their roles in controlling the folding kinetics of β-hairpins (*20*, *21*, *27*−*32*).

So far, a limited number of experiments have attempted to address the question of how folding dynamics vary with the turn (or loop) sequence and length. Consistent with the zipper model of Muñoz et al. (*6*, *27*), Dyer and co-workers (*29*) have recently shown that the folding rate of a β-hairpin could be substantially accelerated when the loop connecting the hydrophobic cluster is made shorter. Similarly, the study of Chan and co-workers also suggested that the turn formation plays an active role in directing β-hairpin folding (*32*). In addition, our recent study on the folding kinetics of a series of 12-residue β-hairpins, which differ only in the amino acid sequence of the putative turn region (*30*), further showed that the entropic penalty associated with the turn (or loop) formation is an important determinant of the free energy barrier of β-hairpin folding. Thus, this observation is in agreement with the computational results of Klimov and Thirumalai (*8*), which showed that the folding speed of β-hairpins depends on the stiffness of the turn.

The kinetic role of the hydrophobic cluster has not been systematically examined, for example, using the method of ϕ-value analysis (*33*). While it was thought that the hydrophobic cluster stabilizes the folding transition state, our study of the folding kinetics of a 16-residue β-hairpin nevertheless suggested that the role of the hydrophobic cluster is largely to prevent the β-sheet strands from unfolding. In other words, the native contacts defining the hydrophobic cluster are formed mostly on the downhill side of the folding free energy barrier (*30*).

These early experimental studies undoubtedly provided new insights into our understanding of the folding mechanism of β-hairpins. However, several important conclusions were reached on the basis of comparisons of folding properties between β-hairpins that differ significantly in sequence. Thus,

[†] Supported by the NIH (Grant GM-065978) and the NSF (Grant CHE-0094077).

* To whom correspondence should be addressed. Telephone: 215-573-6256. Fax: 215-573-2112. E-mail: gai@sas.upenn.edu.

10.1021/bi052039s CCC: $33.50
Published on Web 02/03/2006

Table 1: Name and Sequence of the Peptides Used and Discussed in the Current Study

peptide	sequence
gb1	GEWTYDDATKTFTVTE
trpzip4	GEWTWDDATKTWTWTE
trpzip4-m1	GEWTW**A**DATKTWTWTE
trpzip4-m2	GEWT**Y**DDATKTWTWTE
trpzip4-m3	GEWT**A**DDATKTWTWTE
trpzip4-m4	GEWT**A**DDATKT**A**TWTE
trpzip4-m5	GEWTWD**A**ATKTWTWTE
gb1-m3p	KKWTYNPATGK-Phe$_{CN}$-TVQE

there is a lack of understanding of the β-hairpin folding mechanism at the residue level. Therefore, a thorough study of the folding kinetics of a specific β-hairpin via the commonly used φ-value analysis (*33*) in protein folding will help us not only to verify these conclusions but also to provide a more comprehensive picture regarding the folding mechanism of β-hairpins at the residue level.

For this purpose, we have studied the folding kinetics of several mutants of trpzip4,[1] a 16-residue β-hairpin originally designed by Cochran and co-workers (*34*). As shown (Table 1), trpzip4 is a triple mutant of the gb1 peptide, a widely studied 16-residue β-hairpin derived from the C-terminus of the B1 domain of protein G (*35*). Cochran et al. (*34*) have shown that in aqueous solution trpzip4 adopts a β-hairpin conformation and its thermal folding−unfolding transition follows a two-state process with a thermal melting temperature of about 70 °C. Previously, we have shown that although trpzip4 and the gb1 β-hairpin show quite different thermal stabilities, they fold with similar rates (*30*). While this study revealed a possible kinetic role for the hydrophobic cluster in β-hairpin folding, these results alone are not sufficient to allow us to gain a comprehensive understanding of the folding mechanism of trpzip4. For example, it is not yet known how the transition state is stabilized and what key residues are involved in this process. Clearly, further studies on the folding kinetics of specifically selected trpzip4 mutants are needed in order to provide a better understanding of the nature of the folding transition state of this β-hairpin.

Using a laser-induced temperature-jump infrared (*T*-jump IR) technique (*36*), we studied the folding kinetics of a series of mutants of trpzip4 (Table 1). The D46A mutant (trpzip4-m1) was chosen because the main chain and side chain of Asp46 are found to form a characteristic hydrogen bond network with other residues in the turn region (Figure 1). Since a similar hydrogen bond network existing in the turn region of the gb1 β-hairpin has been shown to play a crucial role in stabilizing its folded state (*13*, *24*), we expect that Asp46 is also important to the stability of trpzip4. Furthermore, because this residue is located at the end of the turn, it is quite likely that it also plays an important role in the formation of the transition state. Therefore, the kinetic role of Asp46 should be examined through mutation. For comparison, we have also studied the folding kinetics of a mutant in which Asp47 was mutated to Ala. To gain a detailed understanding of the role of the hydrophobic cluster in β-hairpin folding, we further studied the following mutants

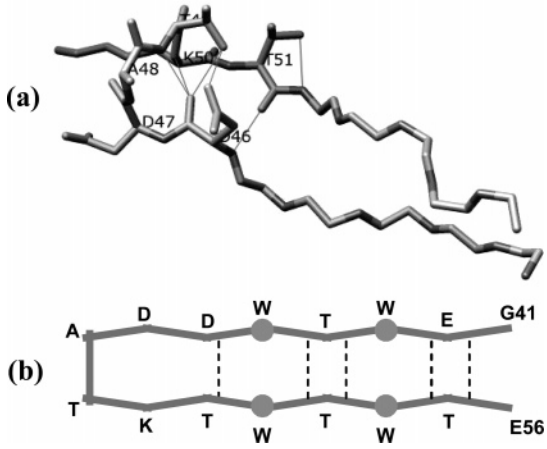

FIGURE 1: (a) Hydrogen bond network of trpzip4 in the turn region. This image was generated using the Chimera program (http://www.cgl.ucsf.edu/chimera) and the NMR structure of trpzip4 (PDB code 1LE3, structure 1). (b) Schematic representation of the backbone conformation of trpzip4. The dashed lines represent the hydrogen bonds.

of trpzip4: W45Y (trpzip4-m2), W45A (trpzip4-m3), and W45A/W52A (trpzip4-m4). Our results showed that Asp46 is indeed crucial not only to the stability but also to the folding rate of trpzip4. Although mutation of the Trp residues also results in a decrease in the stability of trpzip4, the loss of stability is mainly caused by an increase in the unfolding rate. Thus, these results are consistent with our previous study which shows that the turn formation is the rate-limiting step in β-hairpin folding (*30*).

To better understand the nature of the unfolded states of β-hairpins, we have also studied the compactness of the thermally and chaotropically denatured states of a 16-residue β-hairpin, gb1-m3p, using the method of fluorescence resonance energy transfer (FRET). Our results showed that the thermally denatured state of this β-hairpin remains quite compact. However, the urea-denatured state becomes more extended. Taken together, these results suggest that the very first step in β-hairpin formation, when folding begins from an extended conformation, probably corresponds to a process of (hydrophobic) collapse, which leads to the formation of a compact structure. Only in a later step does the native structure emerge, through a searching process within this more compact ensemble.

MATERIALS AND METHODS

The peptides used in the current study were synthesized on the basis of standard Fmoc protocols on a PS3 automated peptide synthesizer (Protein Technologies, Inc., Woburn, MA). All products were purified to homogeneity by reverse-phase chromatography and identified by matrix-assisted laser desorption ionization mass spectroscopy. The residual trifluoroacetic acid (TFA) from peptide synthesis, which has a sharp mid-IR band centered at 1678 cm^{-1}, was removed by multiple lyophilizations against a 0.1 M DCl solution.

Circular dichroism (CD) data were obtained on an Aviv 62A DS spectropolarimeter (Aviv Associates) with a 1 mm sample holder. The peptide concentration was about 40 μM in 20 mM phosphate buffer solution (pH 7). The temperature-dependent ellipticities at 229 nm, i.e., $[\theta](T)$, were further analyzed according to an apparent two-state model, namely

[1] Abbreviations: *T*-jump, temperature jump; FRET, fluorescence resonance energy transfer; TFA, trifluoroacetic acid; CD, circular dichroism; FTIR, Fourier transform infrared; trpzip, tryptophan zipper; FSD, Fourier self-deconvolution.

$$[\theta](T) = \frac{\theta_U(T) + K_{eq}(T)\theta_F(T)}{1 + K_{eq}(T)} \quad (1)$$

$$K_{eq}(T) = \exp(-\Delta G(T)/RT) \quad (2)$$

$$\Delta G(T) = \Delta H_m + \Delta C_p(T - T_m) - T[\Delta S_m + \Delta C_p \ln(T/T_m)] \quad (3)$$

Here, $\theta_F(T)$ is the pretransition baseline, $\theta_U(T)$ is the posttransition baseline, $K_{eq}(T)$ is the folding equilibrium constant, $T_m = \Delta H_m/\Delta S_m$ is the thermal melting temperature, ΔH_m is the enthalpy change at T_m, ΔS_m is the entropy change at T_m, and ΔC_p is the heat capacity change, which has been assumed here to be temperature independent. In the current study, both $\theta_F(T)$ and $\theta_U(T)$ were treated as a linear function of temperature, i.e., $\theta_F(T) = a + bT$ and $\theta_U(T) = c + dT$, where *a*, *b*, *c*, and *d* are constants. In the data analysis, all of the CD thermal melting curves presented in Figure 3 were fit globally, wherein *b* and *d* were treated as global parameters.

Fluorescence spectra were obtained on a Fluorolog 3.10 spectrofluorometer (Jobin Yvon Horiba) with 2 nm spectral resolution (excitation and emission) and a 1 cm quartz sample cuvette. Temperature was regulated using a TLC 50 Peltier temperature controller (Quantum Northwest). The peptide sample was prepared by directly dissolving lyophilized solids into 20 mM phosphate buffer (pH 7), and the final concentration was around 25 μM, determined optically using ϵ_{280} = 850 M^{-1} cm^{-1} for the reference peptide (GK-Phe_{CN}-TV) and ϵ_{280} = 6540 M^{-1} cm^{-1} for gb1-m3p. Temperature-dependent fluorescence spectra (250−450 nm) of gb1-m3p and the reference peptide (GK-Phe_{CN}-TV) were collected from 5 to 95 °C, in a step of 10 °C, with an excitation wavelength of 240 nm. For the urea FRET experiment, the urea concentration of the peptide solution was adjusted using an equimolar peptide (~25 μM) stock solution containing urea (7 M). Each time, an aliquot of the peptide solution was removed from the fluorescence cuvette, followed by the addition of an equal amount of the urea-containing peptide stock solution, resulting in an increase of the urea concentration by 0.75 M.

Temperature-dependent Fourier transform infrared (FTIR) spectra were collected on a Magna-IR 860 spectrometer (Nicolet) using 2 cm^{-1} resolution. A CaF_2 sample cell that was divided into two compartments with a Teflon spacer was used to allow the separate measurements of the sample and the reference under identical conditions. The optical path length of the sample cell was determined to be 52 μm by its interference fringes obtained from the transmittance signal of the empty cell. Temperature control with ±0.2 °C precision was obtained by a thermostated copper block. To reduce the uncertainties induced by slow instrument drifts, both the sample and reference sides of the sample cell were moved in and out of the IR beam alternately, and each time a spectrum corresponding to an average of eight scans was collected. The final result was usually an average of 32 such spectra, both for the sample and for the reference. For both static and time-resolved IR measurements, the sample was prepared by directly dissolving lyophilized solids in 20 mM phosphate and D_2O buffer (pH* 7). The final concentration was typically 1−2 mM, estimated by either the Trp or Tyr absorbance.

The *T*-jump IR setup has been described in detail elsewhere (*37*, *38*). Briefly, a heating pulse at 1.9 μm (3 ns and 10 mJ) was used to generate a *T*-jump of ~10 °C. Transient absorbance change induced by the *T*-jump pulse was probed by a continuous wave IR diode laser and a 50 MHz HgCdTe detector. As in the static FTIR measurement, a sample cell with dual compartments was used to allow the separate measurements of the absorbance change of the sample and reference under identical conditions. The reference measurement provides the information for both background subtraction and *T*-jump amplitude determination. Because the stability of a β-hairpin depends on temperature, a rapid increase in temperature, with the use of an appropriate conformational probe (e.g., IR), allows the measurement of its *T*-jump-induced relaxation kinetics and, thus, the folding and unfolding rates of the system of interest. For a simple two-state scenario, e.g., U ⇔ N (U and N represent the unfolded and the folded states, respectively), it is easy to show that the observed relaxation rate constant is exactly the sum of the folding (k_f) and unfolding (k_u) rate constants. Therefore, the folding and unfolding rate constants can be obtained individually if the equilibrium constant ($K_{eq} = k_f/k_u$) of this two-state reaction at the final temperature is known.

In the FRET study, the FRET efficiency, *E*, was calculated according to the equation (*39*)

$$E = 1 - I_{DA}/I_D \quad (4)$$

where I_{DA} and I_D are the integrated fluorescence intensities of the donor, with and without the presence of the acceptor, respectively. For the current study, I_{DA} corresponds to the integrated area of the Phe_{CN} fluorescence spectrum obtained with the gb1-m3p peptide, and I_D corresponds to that obtained with a pentapeptide, GK-Phe_{CN}-TV, under the same conditions. Here, we have assumed that the Phe_{CN} fluorescence of GK-Phe_{CN}-TV is proportional to that of the gb1-m3 peptide in the absence of FRET. To accurately determine the integrated area of the Phe_{CN} fluorescence, which overlaps the emission spectrum of Trp, we fit the fluorescence spectrum of these peptides by using a linear combination of two profiles generated from fitting the fluorescence spectra of Trp and Phe_{CN} plus a linear background.

RESULTS

CD Spectroscopy. Due to the excitonic coupling between the paired Trp side chains, tryptophan zippers (trpzips) exhibit a unique far-UV CD band centered at ~229 nm (*40*). Similar to that of trpzip4, the far-UV CD spectra of trpzip4-m1, trpzip4-m2, and trpzip4-m5 at 4 °C show substantial positive intensities around 229 nm (Figure 2), indicating that these mutants remain folded at this temperature. In contrast, both trpzip4-m3 and trpzip-m4 lack significant CD intensities at 229 nm (Figure 2), indicating that mutations of the Trp residues significantly compromise the conformational stability of the β-hairpin conformation. Furthermore, the thermal stability of trpzip4-m1, trpzip4-m2, and trpzip4-m5 was quantitatively investigated by monitoring their CD signals at 229 nm as a function of temperature. As shown (Figure 3), the CD thermal unfolding curves of these β-hairpins show characteristics of a cooperative thermal unfolding transition. Compared to trpzip4, however, these data suggest that

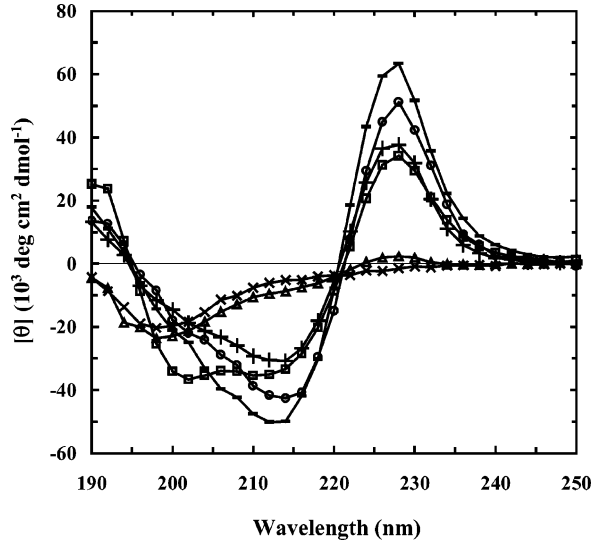

FIGURE 2: CD spectra of trpzip4 (○) (29 μM), trpzip4-m1 (+) (30 μM), trpzip4-m2 (□) (40 μM), trpzip4-m3 (△) (112 μM), trpzip4-m4 (×) (50 μM), and trpzip4-m5 (—) (40 μM) in 20 mM phosphate buffer solution (pH 7) at 4 °C.

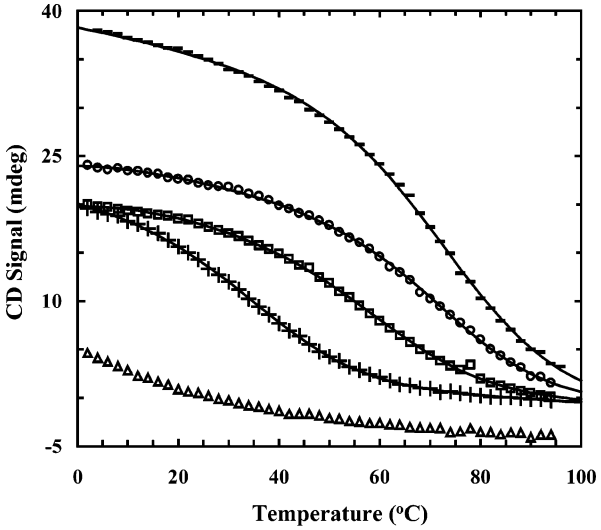

FIGURE 3: CD signals of trpzip4 (○) (29 μM), trpzip4-m1 (+) (30 μM), trpzip4-m2 (□) (40 μM), trpzip4-m3 (△) (112 μM), and trpzip4-m5 (—) (40 μM) in 20 mM phosphate buffer solution (pH 7) at 229 nm as a function of temperature. Smooth lines correspond to fits of these data to a two-state model (i.e., eqs 1−3). The resulting thermodynamic parameters were listed in Table 2.

Table 2: Thermodynamic Folding Parameters Obtained from Equilibrium CD Measurements

peptide	T_m (°C)	ΔH_m (kcal mol^{-1})	ΔS_m (cal K^{-1} mol^{-1})	ΔC_p (cal K^{-1} mol^{-1})
trpzip4	70.4 ± 1.8	−20.2 ± 1.6	−58.8 ± 4.1	−374 ± 35
trpzip4-m1	32.1 ± 0.9	−13.8 ± 0.2	−45.1 ± 2.5	−343 ± 41
trpzip4-m2	61.1 ± 1.2	−15.0 ± 1.4	−45.0 ± 3.7	−307 ± 53
trpzip4-m3	<10			
trpzip4-m4				
trpzip4-m5	71.9 ± 1.4	−18.9 ± 1.1	−54.7 ± 4.7	−245 ± 60

trpzip4-m1 and trpzip4-m2 are less stable. Fitting these CD data globally to a two-state model (i.e., eqs 1−3) yielded those thermodynamic parameters summarized in Table 2. Since only part of the thermal unfolding transition of trpzip4-m3 was observed in the temperature range employed in the current study, we did not attempt to fit its CD data.

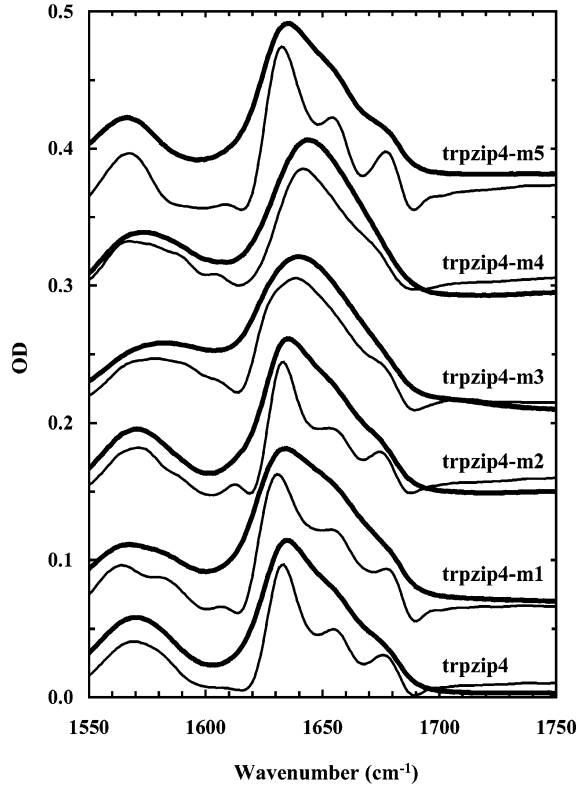

FIGURE 4: FTIR spectra (in the amide I′ region) of trpzip4 and its mutants around 6 °C. Also shown are the corresponding FSD spectra of these data (thinner lines). The band narrowing was achieved by the Fourier self-deconvolution (FSD) method (*41*) with $k = 2$ and fwhm = 18 cm^{-1}. These data have been normalized and offset for clarity.

Nonetheless, this result indicates that the T_m of trpzip4-m3 is less than 10 °C.

Infrared Spectroscopy. FTIR spectroscopy was also employed to study the thermal unfolding transition of these mutants. In particular, the amide I′ bands of these peptides were collected as a function of temperature. Consistent with the results obtained from CD spectroscopy, the amide I′ bands of trpzip4-m1, trpzip4-m2, and trpzip4-m5 at ∼6 °C exhibit characteristic features of antiparallel β-sheets, i.e., the peaks centered at ∼1630 and ∼1680 cm^{-1}, respectively (Figure 4). This pair of bands, which can be seen more clearly from the Fourier self-deconvoluted (FSD) spectra of these peptides, arises from interstrand and intrastrand transition dipole couplings of amide carbonyls and is an established indicator of antiparallel β-sheet structure (*42*−*44*). While the amide I′ bands of these peptides are similar, they show quantitative differences. Theoretical studies have shown that the exact position and intensity of these two coupled bands of β-sheets depend on several factors, such as the relative twist angle and distance between the two β-strands (*45*−*47*). Therefore, the small but apparent differences between these spectra may indicate that the overall β-hairpin conformations adopted by these peptides are slightly different. Also consistent with the CD thermal melting data, the spectral features associated with the folded β-hairpin conformation are gradually melted away with increasing temperature. This is indicated by the negative-going signals centered at ∼1630 and 1678 cm^{-1} in the FTIR difference spectra of trpzip4-m1 (Figure 5). Similarly, the positive-going signal at ∼1660 cm^{-1} in the FTIR difference spectra, which

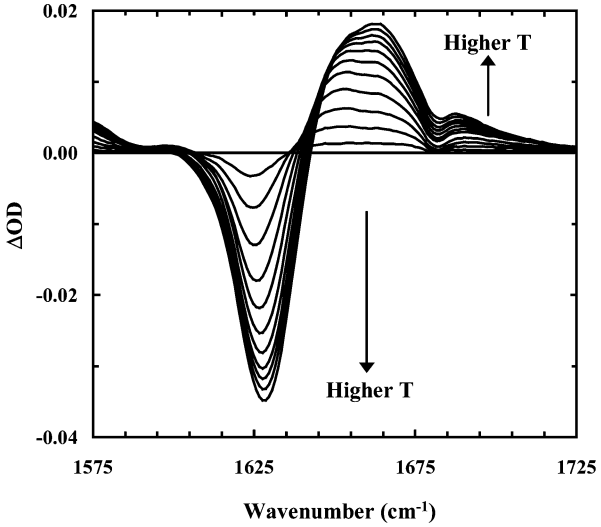

FIGURE 5: Difference FTIR spectra of trpzip4-m1, which were generated by subtracting the spectrum collected at 7.4 °C from those collected at higher temperatures.

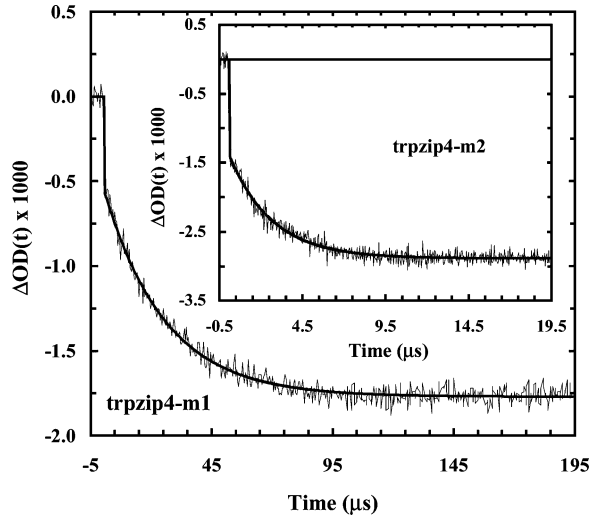

FIGURE 6: Representative relaxation trace of trpzip4-m1 in response to a *T*-jump of about 9 °C, from 20.8 to 30.0 °C. The smooth line is the fit to the function, $\Delta OD(t) = A[1 - B \exp(-t/\tau)]$, with $A = -0.0018$, $B = 0.70$, and $\tau = 25.1$ μs. Also shown (inset) is a representative relaxation trace of trpzip4-m2 in response to a *T*-jump of 5.4 °C, from 50 to 55.4 °C. The smooth line is the fit to the function, $\Delta OD(t) = A[1 - B \exp(-t/\tau)]$, with $A = -0.0029$, $B = 0.54$, and $\tau = 2.6$ μs. The probing frequency was 1630 cm^{-1} for both cases.

arises from the thermally denatured conformations and becomes increasingly more intense at higher temperatures, also shows the thermal unfolding of the β-hairpin structure. In practice, these spectral changes can be used to monitor the *T*-jump-induced conformational kinetics of the β-hairpin of interest (see below).

T-Jump Infrared Study. The folding kinetics of these β-hairpins were studied using the *T*-jump IR technique, wherein a 1.9 μm nanosecond laser pulse is used to rapidly change the temperature of the sample solution. The resulting relaxation kinetics of the β-hairpin of interest were probed by IR spectroscopy. As shown (Figure 6), the *T*-jump-induced relaxation kinetics exhibit two distinct phases. The fast phase is instrumentation limited and is due to temperature-induced spectral changes (*48*−*50*). The slow phase can be fit by a single exponential function and is attributed to the relaxation kinetics of the equilibrium between the folded and thermally denatured β-hairpin conformations. Consistent with the results of other studies (*27*−*30*), the observation here of first-order relaxation kinetics for these β-hairpins indicates that their folding from the thermally denatured state can be described by a two-state process. Thus, using the equilibrium constants obtained from CD and the measured relaxation rate constants, we were able to determine the folding and unfolding rate constants for trpzip4-m1, trpzip4-m2, and trpzip4-m5. As shown (Figure 7), the folding rate of these β-hairpins only weakly depends on temperature, whereas their unfolding rate shows Arrhenius-like temperature dependence, typical to protein unfolding. Moreover, relaxation kinetics obtained using different trpzip4-m1 concentrations (Figure 7) showed that they are independent of the peptide concentration (from approximately 0.5 to 4 mM), further substantiating our assignment that the observed relaxation kinetics arise from the folding and unfolding processes of the β-hairpin conformation.

Because of its low thermal stability, the folding thermodynamics of trpzip4-m3 could not be reliably determined from its thermal unfolding CD data. Therefore, we were unable to uncover its folding rate constant from the measured relaxation rate constant. However, over the temperature range in which the kinetic data were obtained, the observed relaxation rate constant of trpzip4-m3 can be treated approximately as its unfolding rate constant because in this temperature range (10−35 °C) the population of the unfolded state dominates. Interestingly, these results suggest that replacing an aromatic side chain in the hydrophobic cluster with a methyl group substantially increases the unfolding rate of the resultant β-hairpin.

FRET Study. To help to further understand the folding mechanism of β-hairpins, we studied the thermally induced and urea-induced unfolding transitions of a 16-residue β-hairpin, gb1-m3p, using the method of fluorescence resonance energy transfer. The goal is to gain insight into the conformation of the unfolded state and to investigate how the compactness of the denatured state of a β-hairpin depends on the method of denaturation. The gb1-m3 peptide was designed on the basis of the sequence of the gb1 β-hairpin by Andersen and co-workers and has been shown to have a much higher thermal stability than the parent (*26*). To use the method of FRET, we have replaced the single Phe residue in gb1-m3 with a nonnatural amino acid, *p*-cyanophenylalanine (Phe_{CN}). The resulting peptide was named gb1-m3p (Table 1). Tucker et al. have recently shown that Phe_{CN} is an efficient FRET donor to Trp with a Förster distance of about 16 Å and have used this FRET pair to study the conformational distribution of unstructured peptides (*51*).

Our CD results show that the thermal stability of gb1-m3p is comparable to that of gb1-m3, although its unfolding transition becomes less cooperative (data not shown). This is due most likely to the fact that the hydrophobicity of Phe_{CN} is smaller than that of Phe. As shown (Figure 8), the emission spectrum of the gb1-m3p peptide at 20 °C, resulting from a selective excitation of the Phe_{CN} residue at 240 nm, shows features indicative of fluorescence resonance energy transfer. This is further supported by the fluorescence spectra of gb1-m3p obtained in solutions of different urea concentrations. As indicated (Figure 8), the fluorescence intensity of the donor (i.e., Phe_{CN}) increases with the increase of the urea

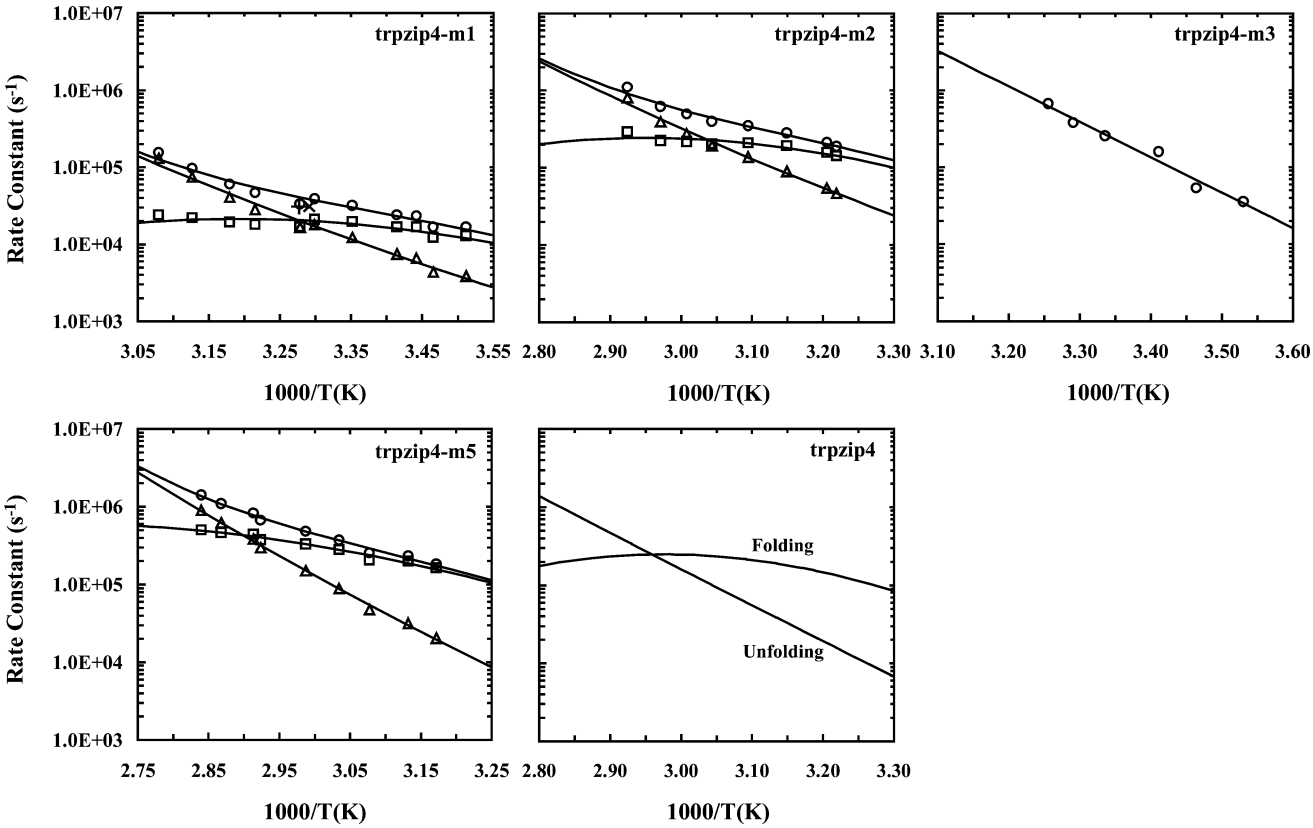

FIGURE 7: Arrhenius plot of the observed relaxation rate constant (○) as well as the folding (□) and unfolding (△) rate constants of trpzip4-m1, trpzip4-m2, and trpzip4-m5, as indicated. For trpzip4-m1, other symbols represent the relaxation rate constants obtained with different peptide concentrations (i.e., + for 0.6 mM and × for 3.9 mM). Lines are fits to the Eyring equation, i.e., $\ln(k) = \ln(D) - \Delta G^{\ddagger}/RT$, where D was set to 1.0×10^{10} s^{-1} and $\Delta G^{\ddagger}$ is temperature-dependent free energy of activation. Also shown are the observed relaxation rate constants of trpzip4-m3 as well as the folding and unfolding rate constants of trpzip4 (derived from ref *30*).

concentration, indicating that as the β-hairpin conformation unfolds at higher concentrations of denaturant, the FRET efficiency decreases, as a result of the increased separation distance between the FRET donor (Phe_{CN}) and acceptor (Trp). It should be noted, however, that the intensity of the Trp emission should not be used as a quantitative measure of the FRET efficiency because several amino acids in this peptide, such as Lys and Gln, can quench the Trp fluorescence (*52*).

Using this FRET pair, we were able to monitor the thermally induced and chaotropically induced unfolding transitions of gb1-m3p. As shown (Figure 9), the apparent FRET efficiency calculated using the method described in the Materials and Methods section was found to be independent of the peptide concentration (between 25 and 250 μM). Furthermore, the FRET efficiency decreases with the increase of either the temperature or the concentration of urea, indicating that the average distance between Phe_{CN} and Trp increases as the β-hairpin conformation unfolds. Interestingly, however, these results suggest that the thermally unfolded state of gb1-m3p is more compact than its urea-denatured state. For example, the FRET efficiency only changes from ~90% to ~60% when the temperature is changed from 5 to 95 °C, where the β-hairpin population is very small according to CD spectroscopy, whereas in 6.75 M urea the FRET efficiency reduces to about 40%.

DISCUSSION

It is well recognized that a stable β-hairpin structure results from an intricate interplay among several factors, including hydrogen bonding, electrostatic interaction, turn preference (sequence), and hydrophobic packing of side chains (*22*−*26*). For example, a commonly used strategy in β-hairpin design is to use a hydrophobic cluster, formed by several cross-strand hydrophobic side chains, to stabilize the folded conformation (*35*, *53*−*55*). Recently, Cochran and co-workers (*34*) have shown that a combination of two Trp-Trp non-hydrogen-bonded cross-strand pairs is generally useful in stabilizing β-hairpin structures. They have used this tryptophan zipper structural motif in several peptides, including trpzip4, and showed that these peptides fold into a β-hairpin structure in which the paired Trp side chains adopt an edge-to-face geometry. A recent computational study by Brooks and co-workers (*56*) indicated that this type of Trp side chain orientation found in the trpzips could be attributed mainly to the electrostatic multipole moments of the indole ring. Because of the strong and favorable interaction between the paired Trp side chains, trpzip4 exhibits thermodynamic properties similar to those of proteins (*34*). Therefore, it is expected that mutation of each one of the four Trp residues would lead to a decrease in the thermal stability of the β-hairpin conformation. Consistent with this expectation, our equilibrium studies show that mutation of Trp45 to Tyr results in a decrease in the T_m by ~9 °C, while the effect of mutation of Trp45 to Ala is even more drastic. The CD and IR data of trpzip4-m3 suggest that at room temperature the population of its folded state is quite small. Although we were unable to quantitatively determine the folding−unfolding thermodynamics of trpzip4-m3, it is apparent that its T_m is lower than 10 °C (Figure 3). Finally, when two Trp

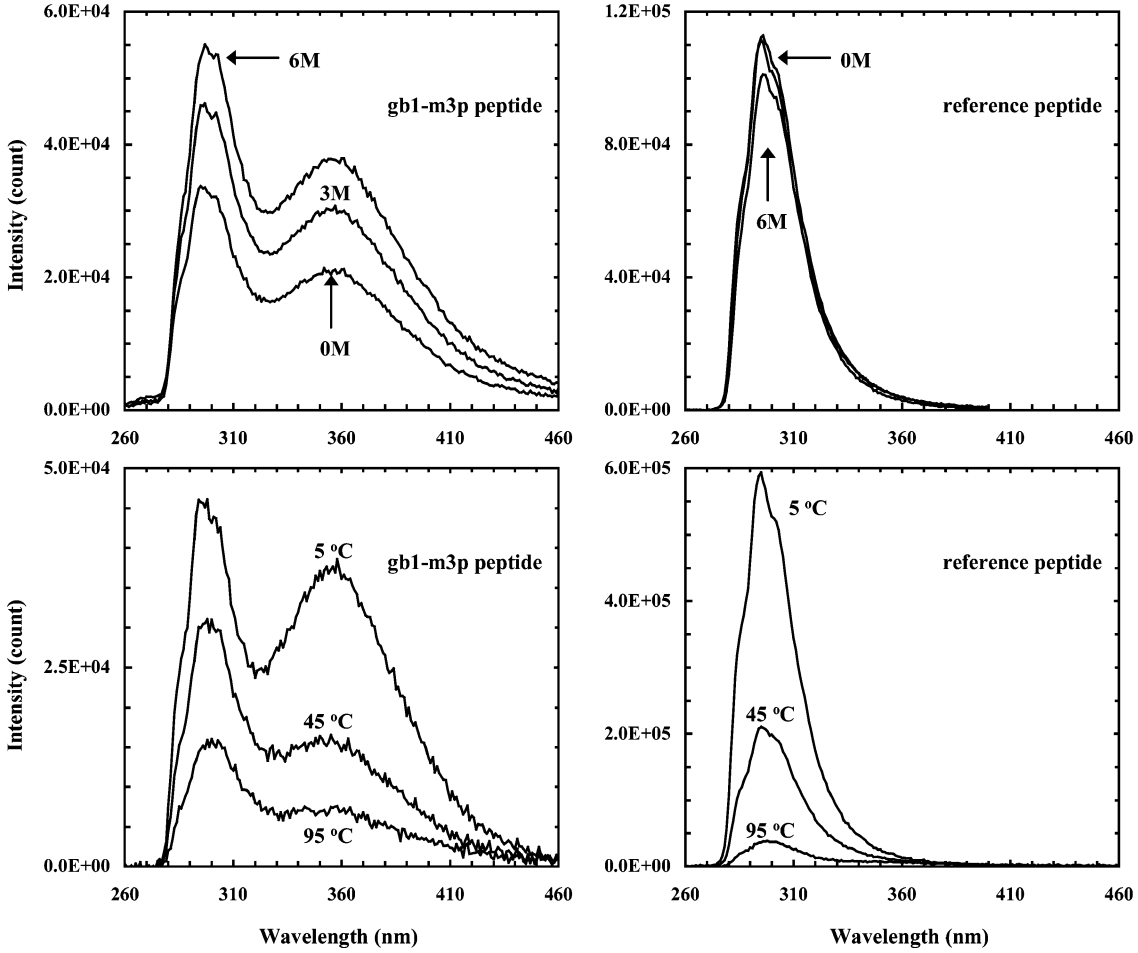

FIGURE 8: Upper panel: Fluorescence spectra of gb1-m3p (25 μM) and the reference peptide (25 μM) at 20.0 °C as a function of the urea concentration, as indicated. Lower panel: Fluorescence spectra of gb1-m3p (25 μM) and the reference peptide (25 μM) collected at different temperatures, as indicated. An excitation wavelength of 240 nm was used in these experiments.

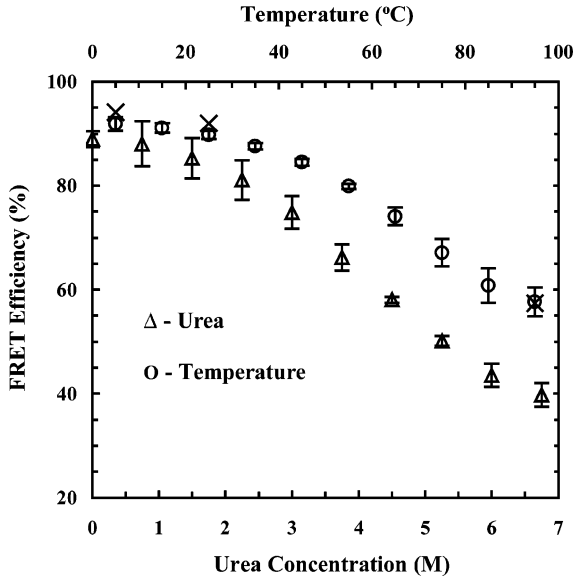

FIGURE 9: FRET efficiency of gb1-m3p vs temperature (○) and urea concentration (△). The peptide concentration was 25 μM. Also shown are FRET efficiencies (×) obtained with a peptide concentration of 250 μM. The urea data were collected at 20.0 °C.

residues were mutated to Ala, the resulting peptide (i.e., trpzip4-m4) yielded no detectable β-hairpin population at room temperature. These results further highlight the importance of Trp residues in maintaining the stability of the trpzip β-hairpins. Similarly, it has been shown that for the gb1 β-hairpin the hydrophobic cluster also largely contributes to the stability of the native structure (*24*). For example, mutation of Tyr45 to Ala strongly destabilizes the gb1 β-hairpin.

Apparently, the turn (loop) sequence is another important determinant of β-hairpin stability. For example, in the design of stable β-hairpins, D-Pro is commonly employed to increase the turn propensity (*23*) and, consequently, the stability of the β-hairpin. The reason is that D-Pro is conformationally rigid and, therefore, can decrease the entropic cost associated with the turn formation. Similarly, interactions that can restrict the flexibility of the turn are also very important. For example, Frank et al. (*57*) have shown that even in 7.4 M urea the B1 domain of protein G still shows residual structures that involve Asp46, Thr49, and Thr51, indicating that the loop region of the GB1 second β-hairpin is quite stable and rigid and, thus, beneficial for folding. The study of Baker and co-workers (*58*) further showed that mutations of Asp46 and Thr49 to Ala dramatically decrease the folding rate of the B1 domain of protein G, indicating that the rigidity of this loop is also crucial to the folding kinetics of this protein.

Recently, Munekata et al. (*24*) have shown that a characteristic hydrogen bond network in the loop region of the gb1 β-hairpin, which involves mostly Asp46, Thr49, and Lys50, is important for its stability because most single

Table 3: Folding and Unfolding Time Constants of trpzips and the gb1 Peptide at 45 °C and ϕ-Values of trpzip4-m1, -m2, and -m5

peptide	τ_f at 45 °C (μs)	τ_u at 45 °C (μs)	ϕ-value
trpzip4	5.4 ± 0.4	28.5 ± 1.2	
trpzip4-m1	46.9 ± 2.3	16.3 ± 2.0	0.77 ± 0.04
trpzip4-m2	5.4 ± 0.6	11.2 ± 0.9	0.0 ± 0.12
trpzip4-m3		~0.5	
trpzip4-m5	5.6 ± 0.4	37.6 ± 1.5	0.0 ± 0.15
gb1[a]	6.2	1.8	

[a] Adopted from the study of Muñoz et al. (*27*).

mutations in this region destabilize the β-hairpin conformation. They further pointed out that the reason that this hydrogen bond network plays a stabilizing role in the folding of the gb1 β-hairpin is that it is particularly crucial for maintaining the rigidity of the loop by restricting rotational freedoms of the main chain and/or the side chains (*24*). Using molecular dynamics simulations, Tsai and Levitt have reached a similar conclusion (*13*). Since a similar hydrogen bond network also exists in the loop region of trpzip4 (Figure 1), wherein Asp46 is mostly involved, it is therefore expected that mutation of this residue to Ala will affect the stability of the β-hairpin conformation. Indeed, the thermal stability of trpzip4-m1 is significantly decreased as compared to that of trpzip4, indicating that Asp46 plays a crucial stabilizing role in trpzip4. This is consistent with the experimental result of Munekata et al. (*24*) and also the simulation result of Tsai and Levitt (*13*). On the contrary, mutating Asp47 to Ala results in a slight increase in the thermal melting temperature of the β-hairpin (*24*), further corroborating the idea that Asp46 plays a unique role in the folding of trpzip4 and the gb1 β-hairpin.

Microscopically, the stability of the folded state of a two-state folder is controlled by both the folding and unfolding rates. For example, a decrease in stability can result from a decrease in the folding rate, an increase in the unfolding rate, or both. Therefore, studying the folding−unfolding kinetics of these trpzip4 mutants will shed light on the question of kinetically what controls the conformational stability of trpzip4. Moreover, it will help to delineate the molecular mechanism of β-hairpin folding.

The folding kinetics of these peptides were studied by the *T*-jump initiation technique in conjunction with infrared spectroscopy. The folding rates obtained in the temperature range of the data measured are comparable to those observed for other β-hairpins (*27*−*31*, *59*). However, comparisons between the folding−unfolding rates of these β-hairpins revealed that mutations in the loop and hydrophobic cluster regions result in different effects on the folding kinetics. For example, when Trp45 was mutated to either Tyr or Ala, the folding rate of the resulting mutant is almost identical to that of the wild type, whereas its unfolding rate increases (Figure 6 and Table 3). For example, at 45 °C (*60*) the folding rates of trpzip4 and trpzip4-m2 are $(5.4 \pm 0.4\ \mu s)^{-1}$ and $(5.4 \pm 0.6\ \mu s)^{-1}$, respectively, whereas their unfolding rates are $(28.5 \pm 1.2\ \mu s)^{-1}$ and $(11.2 \pm 0.9\ \mu s)^{-1}$, respectively. Thus, the ϕ-value of trpzip4-m2 is practically zero at this temperature, suggesting that the native contacts involving Trp45 are not developed at the folding transition state. Consistent with this picture, the unfolding rate of trpzip4-m3 becomes even faster. As shown (Figure 7), the unfolding rate of trpzip4-m3 is estimated to be about $(0.5\ \mu s)^{-1}$ at 45 °C, approximately 56 times faster than that of the wild-type trpzip4. For trpzip4-m4, its unfolding rate is probably even more rapid than that of trpzip4-m3 because there is no detectable β-hairpin population at even the lowest temperature employed in the current study. In agreement with our early conclusion (*30*), these results therefore suggest that the major kinetic role of the hydrophobic cluster is to prevent the β-hairpin conformation from unfolding, primarily by decreasing its unfolding rate. Thus, any mutations that decrease the cohesive strength of the hydrophobic cluster will lead to an increase in the unfolding rate and, as a result, a decrease in the conformational stability of the β-hairpin. On the other hand, these results also show that mutations which change the hydrophobic cluster do not significantly affect the folding rate, suggesting that most of the native contacts between those hydrophobic side chains are formed after the folding transition state. Consistent with this picture, Searle and co-workers have shown that the β-strand has a natural predisposition to adopt an extended conformation in the absence of secondary structure interactions (*53*). Thus, the folding process, which may be viewed as the coalescence of two preformed "rigid rods", would be insensitive to mutations in the β-strand.

Previously, we have shown that the formation of the turn (or loop) is the rate-limiting step in β-hairpin folding (*30*). The kinetic results obtained on trpzip4-m1 are thus supportive of this mechanism. As discussed above, Asp46 is crucial to the stability of trpzip4 because both its main chain and side chain are involved in the formation of a characteristic hydrogen bond network in the turn region, similar to that found in the gb1 β-hairpin. Therefore, mutations that can disrupt this hydrogen bond network will change the folding rate, provided that this hydrogen bond network is fully or even partially formed in the folding transition state. Indeed, our results show that mutating Asp46 to Ala leads to a significant decrease in the folding rate (by approximately 9 times) and also a large ϕ-value (~0.77 at 45 °C), whereas mutating Asp47 to Ala results in only a minor change in the folding rate and, consequently, a small ϕ-value. Unlike those amino acid side chains packed in the core region of a protein, the side chain of a residue (e.g., Asp47) in the turn region of a β-hairpin may be dynamic and lacks well-defined interactions with other amino acids. Therefore, one should take extra care in interpreting the experimental ϕ-values. Nevertheless, these results indicate that Asp46 plays a key role in stabilizing not only the native turn conformation but also the folding transition state. This picture is consistent with the conclusion reached by Tsai and Levitt (*13*), who pointed out that the hydrogen bonds in the turn region of the gb1 peptide most likely help to guide correct turn formation in this β-hairpin. Moreover, the unfolding rate of trpzip4-m1 is approximately doubled compared to that of trpzip4, suggesting that the characteristic hydrogen bond network associated with Asp46 is only partially formed at the transition state or that the mutation of Asp46 to Ala weakens the hydrophobic packing, resulting in a faster unfolding rate.

The results obtained here are consistent with the zipper model of Muñoz et al. (*6*, *27*), which emphasizes the initiating role of the turn in β-hairpin folding. However, the ϕ-value analysis allowed us to pinpoint those interactions that stabilize the conformation of the transition state. Clearly,

our results suggest that for trpzip4 (probably it is also true for the gb1 peptide) Asp46 plays a key role in stabilizing the transition state. Apparently, the formation of the characteristic hydrogen bond network associated with Asp46 and other turn residues can significantly decrease the folding free energy barrier and, consequently, increase the folding rate. On the other hand, the near-zero ϕ-value obtained with trpzip4-m2 and also the significantly increased unfolding rate observed for trpzip4-m3 suggest that the hydrophobic cluster has a rather small effect on the energetics of the transition state (when folding proceeds from the thermally denatured states).

A large number of stopped-flow folding studies have shown that an initial collapse process occurs before the main folding kinetics (*61*−*63*). While ample evidence suggests that this process is driven by hydrophobic interactions, which lead to the formation of a compact "denatured state" from which the native state emerges, it is not clear if such a process always favorably guides folding (*64*). One view is that this initial collapse process effectively reduces the conformational space that a protein has to search, therefore, speeding up folding. On the contrary, some studies have shown that an initial collapse process may actually slow folding. Since several computational studies (*7*, *11*, *12*, *16*) have indicated that the first step in β-hairpin formation is a process of hydrophobic collapse (when the folding simulation starts from an extended conformation), we have examined the thermally induced and urea-induced unfolding transitions of a 16-residue β-hairpin (gb1-m3p) using the technique of FRET with the aim of elucidating if such a collapse process exists on the folding pathway of β-hairpins. While the FRET technique has been used in the study of the folding−unfolding transition of other β-sheet proteins and β-hairpins (*65*, *66*), the major distinction between our method and those used in other studies is that we employed two amino acids as the FRET pair (i.e., Phe_{CN} and Trp), and therefore, the perturbation to the native structure is minimized. For small peptides and proteins, introducing a bulky dye FRET pair into their sequence may significantly affect their folding properties.

Our results indicate that even at 95 °C, where most of the gb1-m3p molecules are presumably unfolded according to CD spectroscopy, the apparent FRET efficiency is still very high (∼60%). This result suggests that the thermally unfolded state of gb1-m3p is quite compact because the Förster distance of the FRET pair employed in the current study is only about 16 Å. However, in 6.75 M urea, the FRET efficiency is reduced to ∼40% at 20 °C, indicating that the urea-denatured state of gb1-m3p becomes more extended. For comparison, it is worth noting that a fully extended gb1-m3p would give rise to a FRET efficiency of ∼5%. The observation here that the gb1-m3p β-hairpin adopts a compact thermally unfolded state is certainly interesting, but not surprising. Similar behaviors have also been observed for other peptides and proteins (*51*, *57*, *67*−*69*). For example, Gruebele and co-workers (*67*), who studied the conformational changes of one of the tryptophan zippers (trpzip2) as a function of temperature and concentration of urea using both spectroscopic methods and molecular dynamics simulation, have shown that the thermally denatured states of trpzip2 are clearly more ordered without the presence of chemical denaturant.

The implication of these FRET results is that the very first step along the folding pathway of β-hairpin is a collapse process, probably hydrophobic in nature, provided the initial conformation is extended. Since the process of hydrophobic collapse has been shown to occur on the nanosecond time scale (*70*), an initial hydrophobic collapse process in β-hairpin formation may speed up the rate of folding because it can narrow the conformational space that must be searched associated with the formation of the turn (or loop). Interestingly, we recently observed that the folding rate of the cold-denatured state of a 16-residue β-hairpin is slightly slower than that of its heat-denatured state (*59*). Given the fact that the strength of hydrophobic interactions decreases with decreasing temperature, this result is thus not entirely unexpected because the cold-denatured state may become slightly more extended than the heat-denatured state.

Taken together, these results suggest a comprehensive β-hairpin folding mechanism wherein the initial step corresponds to a collapse process if the denatured state assumes a highly extended conformation, which is followed by the formation of the turn (or loop), and then the consolidation of the native strands in which most of the native contacts between hydrophobic side chains are only formed at the downhill side of the free energy barrier. While the turn formation is shown to be the rate-limiting step, it is worth pointing out that here the turn formation should be regarded as a process wherein the dihedral angles of the backbone are locked into their native values, whereas individual side chains may or may not be placed in their native conformations. Finally, it is also worth pointing out that mutations in the turn region could also lead to a significant change in the unfolding rate if such a mutation affects the native packing of the strands, such as those resulting from cross-strand hydrophobic and electrostatic interactions. Similarly, the folding rate could also be affected if a mutation in the β-strand affects the unfolded state. Therefore, one should be cautious when interpreting the effect of a mutation to the folding kinetics of β-hairpins.

CONCLUSION

The folding thermodynamics and kinetics of a series of mutants of trpzip4 were studied using spectroscopic methods. Our results indicated that Asp46 plays a crucial role in stabilizing the folding transition state of trpzip4, suggesting that the turn (or loop) formation is the rate-limiting step in β-hairpin folding. On the other hand, mutations at the hydrophobic cluster region were found to mostly affect the unfolding rate, further suggesting that the role of the hydrophobic cluster is to prevent the native β-hairpin conformation from unfolding, which substantiates our previous conclusions (*30*). In addition, our FRET study indicated that the thermally denatured state of a 16-residue β-hairpin (gb1-m3p) is much more compact than the urea-denatured state. The implication of this finding is that when folding proceeds from an extended conformation, the very first step probably corresponds to a collapse process.

REFERENCES

1. Searle, M. S., and Ciani, B. (2004) Design of β-sheet systems for understanding the thermodynamics and kinetics of protein folding, *Curr. Opin. Struct. Biol. 14*, 458−464.

2. Gellman, S. H. (1998) Minimal model systems for β sheet secondary structure in proteins, *Curr. Opin. Chem. Biol. 2*, 717−725.
3. Serrano, L. (2000) The relationship between sequence and structure in elementary folding units, *Adv. Protein Chem. 53*, 49−85.
4. Searle, M. S. (2001) Peptide models of protein β-sheets: design, folding and insights into stabilising weak interactions, *J. Chem. Soc., Perkin Trans. 2*, 1011−1020.
5. Pande, V. S., and Rokhsar, D. S. (1999) Molecular dynamics simulations of unfolding and refolding of a β-hairpin fragment of protein G, *Proc. Natl. Acad. Sci. U.S.A. 96*, 9062−9067.
6. Muñoz, V., Henry, E. R., Hofrichter, J., and Eaton, W. A. (1998) A statistical mechanical model for β-hairpin kinetics, *Proc. Natl. Acad. Sci. U.S.A. 95*, 5872−5879.
7. Dinner, A. R., Lazaridis, T., and Karplus, M. (1999) Understanding β-hairpin formation, *Proc. Natl. Acad. Sci. U.S.A. 96*, 9068−9073.
8. Klimov, D. K., and Thirumalai, D. (2000) Mechanisms and kinetics of β-hairpin formation, *Proc. Natl. Acad. Sci. U.S.A. 97*, 2544−2549.
9. Bonvin, A. M. J. J., and van Gunsteren, W. F. (2000) β-Hairpin stability and folding: molecular dynamics studies of the first β-hairpin of Tendamistat, *J. Mol. Biol. 296*, 255−268.
10. Zhou, R., Berne, B. J., and Germain, R. (2001) The free energy landscape for β-hairpin folding in explicit water, *Proc. Natl. Acad. Sci. U.S.A. 98*, 14931−14936.
11. García, A. E., and Sanbonmatsu, K. Y. (2001) Exploring the energy landscape of a β-hairpin in explicit solvent, *Proteins 42*, 345−354.
12. Zhou, Y., and Linhananta, A. (2002) Role of hydrophilic and hydrophobic contacts in folding of the second β-hairpin fragment of protein G: molecular dynamics simulation studies of an all-atom model, *Proteins 47*, 154−162.
13. Tsai, J., and Levitt, M. (2002) Evidence of turn and salt bridge contributions to β-hairpin stability: MD simulations of C-terminal fragment from the B1 domain of protein G, *Biophys. Chem. 101*−*102*, 187−201.
14. Wu, X., Wang, S., and Brooks, B. R. (2002) Direct observation of the folding and unfolding of a β-hairpin in explicit water through computer simulation, *J. Am. Chem. Soc. 124*, 5282−5283.
15. Ma, B., and Nussinov, R. (2003) Energy landscape and dynamics of the β-hairpin G peptide and its isomers: topology and sequences, *Protein Sci. 12*, 1882−1893.
16. Bolhuis, P. G. (2003) Transition-path sampling of β-hairpin folding, *Proc. Natl. Acad. Sci. U.S.A. 100*, 12129−12134.
17. Snow, C. D., Qiu, L., Du, D., Gai, F., Hagen, S. J., and Pande, V. S. (2004) Trp zipper folding kinetics by molecular dynamics and temperature-jump spectroscopy, *Proc. Natl. Acad. Sci. U.S.A. 101*, 4077−4082.
18. Paschek, D., and García, A. E. (2004) Reversible temperature and pressure denaturation of a protein fragment: a replica exchange molecular dynamics simulation study, *Phys. Rev. Lett. 93*, 2381−2405.
19. Krivov, S. V., and Karplus, M. (2004) Hidden complexity of free energy surfaces for peptide (protein) folding, *Proc. Natl. Acad. Sci. U.S.A. 101*, 14766−14770.
20. Kuo, N. N.-W., Huang, J. J.-T., Miksovska, J., Chen, R. P.-Y., Larsen, R. W., and Chan, S. I. (2005) Effects of turn stability on the kinetics of refolding of a hairpin in a β-sheet, *J. Am. Chem. Soc. 127*, 16945−16954.
21. Olsen, K. A., Fesinmeyer, R. M., Stewart, J. M., and Andersen, N. H. (2005) Hairpin folding rates reflect mutations within and remote from the turn region, *Proc. Natl. Acad. Sci. U.S.A. 102*, 15483−15487.
22. Blanco, F. J., Ramirez-Alvarado, M., and Serrano, L. (1998) Formation and stability of β-hairpin structures in polypeptides, *Curr. Opin. Struct. Biol. 8*, 107−111.
23. Espinosa, J. F., Syud, F. A., and Gellman, S. H. (2002) Analysis of the factors that stabilize a designed two-stranded antiparallel β-sheet, *Protein Sci. 11*, 1492−1505.
24. Kobayashi, N., Honda, S., Yoshii, H., and Munekata, E. (2000) Role of side-chains in the cooperative β-hairpin folding of the short C-terminal fragment derived from streptococcal protein G, *Biochemistry 39*, 6564−6571.
25. Espinosa, J. F., Muñoz, V., and Gellman, S. H. (2001) Interplay between hydrophobic cluster and loop propensity in β-hairpin formation, *J. Mol. Biol. 306*, 397−402.
26. Fesinmeyer, R. M., Hudson, F. M., and Andersen, N. H. (2004) Enhanced hairpin stability through loop design: the case of the protein GB1 domain hairpin, *J. Am. Chem. Soc. 126*, 7238−7243.
27. Muñoz, V., Thompson, P. A., Hofrichter, J., and Eaton, W. A. (1997) Folding dynamics and mechanism of β-hairpin formation, *Nature 390*, 196−199.
28. Xu, Y., Oyola, R., and Gai, F. (2003) Infrared study of the stability and folding kinetics of a 15-residue β-**hairpin**, *J. Am. Chem. Soc. 125*, 15388−15394.
29. Dyer, R. B., Maness, S. J., Peterson, E. S., Franzen, S., Fesinmeyer, R. M., and Andersen, N. H. (2004) The mechanism of β-hairpin formation, *Biochemistry 43*, 11560−11566.
30. Du, D., Zhu, Y., Huang, C.-Y., and Gai, F. (2004) Understanding the key factors that control the rate of β-hairpin folding, *Proc. Natl. Acad. Sci. U.S.A. 101*, 15915−15920.
31. Yang, W. Y., and Gruebele, M. (2004) Detection-dependent kinetics as a probe of folding landscape microstructure, *J. Am. Chem. Soc. 126*, 7758−7759.
32. Chen, R. P., Huang, J. J., Chen, H.-L., Jan, H., Velusamy, M., Lee, C., Fann, W., Larsen, R. W., and Chan, S. I. (2004) Measuring the refolding of β-sheets with different turn sequences on a nanosecond time scale, *Proc. Natl. Acad. Sci. U.S.A. 101*, 7305−7310.
33. Matouschek, A., Kellis, J. T., Serrano, L., and Fersht, A. R. (1989) Mapping the transition state and pathway of protein folding by protein engineering, *Nature 340*, 122−126.
34. Cochran, A. G., Skelton, N. J., and Starovasnik, M. A. (2001) Tryptophan zippers: stable, monomeric β-hairpins, *Proc. Natl. Acad. Sci. U.S.A. 98*, 5578−5583.
35. Blanco, F. J., Rivas, G., and Serrano, L. (1994) A short linear peptide that folds into a native stable β-hairpin in aqueous solution, *Nat. Struct. Biol. 1*, 584−590.
36. Zhu, Y., Wang, T., and Gai, F. (2005) Laser-induced *T*-jump method, a nonconventional photo-releasing approach to study protein folding, in *Dynamic Studies in Biology: Phototriggers, Photoswitches and Caged Biomolecules* (Goeldner, G., and Givens, R., Eds.) pp 461−478, Wiley-VCH Verlag GmbH, Weinheim.
37. Huang, C.-Y., Klemke, J. W., Getahun, Z., DeGrado, W. F., and Gai, F. (2001) Temperature-dependent helix-coil transition of an alanine based peptide, *J. Am. Chem. Soc. 123*, 9235−9238.
38. Huang, C.-Y., Getahun, Z., Zhu, Y., Klemke, J. W., DeGrado, W. F., and Gai, F. (2002) Helix formation via conformation diffusion search, *Proc. Natl. Acad. Sci. U.S.A. 99*, 2788−2793.
39. Steinberg, I. Z. (1971) Long-range nonradiative transfer of electronic excitation energy in proteins and polypeptides, *Annu. Rev. Biochem. 40*, 83−114.
40. Grishina, I. B., and Woody, R. W. (1994) Contributions of tryptophan side chains to the circular dichroism of globular proteins: exciton couplets and coupled oscillators, *Faraday Discuss. 99*, 245−262.
41. Kauppinen, J. K., Moffatt, D. J., Mantsch, H. H., and Cameron, D. G. (1981) Fourier self-deconvolution: a method for resolving intrinsically overlapped bands, *Appl. Spectrosc. 35*, 271−276.
42. Krimm, S., and Abe, Y. (1972) Intermolecular interaction effects in the amide I vibrations of β-polypeptides, *Proc. Natl. Acad. Sci. U.S.A. 69*, 2788−2792.
43. Moore, W. H., and Krimm, S. (1975) Transition dipole coupling in amide I modes of β-polypeptides, *Proc. Natl. Acad. Sci. U.S.A. 72*, 4933−4935.
44. Wang, T., Xu, Y., Du, D., and Gai, F. (2004) Determining β-sheet stability by Fourier transform infrared difference spectra, *Biopolymers 75*, 163−172.
45. Choi, J.-H., Ham, S., and Cho, M. (2003) Local amide I mode frequencies and coupling constants in polypeptides, *J. Phys. Chem. B 107*, 9132−9138.
46. Paul, C., Wang, J., Wimley, W. C., Hochstrasser, R. M., and Axelsen, P. H. (2004) Vibrational coupling, isotopic editing, and β-sheet structure in a membrane-bound polypeptide, *J. Am. Chem. Soc. 126*, 5843−5850.
47. Bour, P., and Keiderling, T. A. (2004) Structure, spectra and the effects of twisting of β-sheet peptides. A density functional theory study, *THEOCHEM 675*, 95−105.
48. Volk, M., Kholodenko, Y., Lu, H. S. M., Gooding, E. A., DeGrado, W. F., and Hochstrasser, R. M. (1997) Peptide conformational dynamics and vibrational Stark effects following photoinitiated disulfide cleavage, *J. Phys. Chem. B 101*, 8607−8616.
49. Zhu, Y., Fu, X., Wang, T., Tamura, A., Takada, S., Saven, J. G., and Gai, F. (2004) Guiding the search for a protein's maximum rate of folding, *Chem. Phys. 307*, 99−109.
50. Bredenbeck, J., Helbing, J., Kumita, J. R., Woolley, G. A., and Hamm, P. (2005) α-Helix formation in a photoswitchable peptide

tracked from picoseconds to microseconds by time-resolved IR spectroscopy, *Proc. Natl. Acad. Sci. U.S.A. 102*, 2379−2384.
51. Tucker, M. J., Oyola, R., and Gai, F. (2005) Conformational distribution of a 14-residue peptide in solution: a fluorescence resonance energy transfer study, *J. Phys. Chem. B 109*, 4788−4795.
52. Chen, Y., and Barkley, M. D. (1998) Toward understanding tryptophan fluorescence in proteins, *Biochemistry 37*, 9976−9982.
53. Maynard, A. J., Sharman, G. J., and Searle, M. S. (1998) Origin of β-hairpin stability in solution: structural and thermodynamic analysis of the folding of a model peptide supports hydrophobic stabilization in water, *J. Am. Chem. Soc. 120*, 1996−2007.
54. Espinosa, J. F., and Gellman, S. H. (2000) A designed β-hairpin containing a natural hydrophobic cluster, *Angew. Chem., Int. Ed. 39*, 2330−2333.
55. Tatko, C. D., and Waters, M. L. (2002) Selective aromatic interactions in β-hairpin peptides, *J. Am. Chem. Soc. 124*, 9372−9373.
56. Guvench, O., and Brooks, C. L., III (2005) Tryptophan side chain electrostatic interactions determine edge-to-face vs parallel-displaced tryptophan side chain geometries in the designed β-hairpin "trpzip2", *J. Am. Chem. Soc. 127*, 4668−4674.
57. Frank, M. K., Clore, G. M., and Gronenborn, A. M. (1995) Structural and dynamic characterization of the urea denatured state of the immunoglobulin binding domain of streptococcal protein G by multidimensional heteronuclear NMR spectroscopy, *Protein Sci. 4*, 2605−2615.
58. McCallister, E. L., Alm, E., and Baker, D. (2000) Critical role of β-hairpin formation in protein G folding, *Nat. Struct. Biol. 7*, 669−673.
59. Xu, Y., Wang, T., and Gai, F. (2005) Strange temperature dependence of the folding rate of a 16-residue β-hairpin, *Chem. Phys.* (published online Oct 4, 2005).
60. The reason that we compare the folding/unfolding rates of trpzip4 and its mutants at this temperature is that comparison can be made between experimental data (not extrapolated).
61. Ferguson, N., and Fersht, A. R. (2003) Early events in protein folding, *Curr. Opin. Struct. Biol. 13*, 75−81.
62. Magg, C., and Schmid, F. X. (2004) Rapid collapse precedes the fast two-state folding of the cold shock protein, *J. Mol. Biol. 335*, 1309−1323.
63. Arai, M., Ito, K., Inobe, T., Nakao, M., Maki, K., Kamagata, K., Kihara, H., Amemiya, Y., and Kuwajima, K. (2002) Fast compaction of α-lactalbumin during folding studied by stopped-flow x-ray scattering, *J. Mol. Biol. 321*, 121−132.
64. Roder, H., and Colón, W. (1997) Kinetic role of early intermediates in protein folding, *Curr. Opin. Struct. Biol. 7*, 15−28.
65. Kuznetsov, S. V., Hilario, J., Keiderling, T. A., and Ansari, A. (2003) Spectroscopic studies of structural changes in two β-sheet-forming peptides show an ensemble of structures that unfold noncooperatively, *Biochemistry 42*, 4321−4332.
66. Schuler, B., Lipman, E. A., and Eaton, W. A. (2002) Probing the free-energy surface for protein folding with single-molecule fluorescence spectroscopy, *Nature 419*, 743−747.
67. Yang, W. Y., Pitera, J. W., Swope, W. C., and Gruebele, M. (2004) Heterogeneous folding of the trpzip hairpin: full atom simulation and experiment, *J. Mol. Biol. 336*, 241−251.
68. Luisi, D. L., Wu, W. J., and Raleigh, D. P. (1999) Conformational analysis of a set of peptides corresponding to the entire primary sequence of the N-terminal domain of the ribosomal protein L9: Evidence for stable native-like secondary structure in the unfolded state, *J. Mol. Biol. 287*, 395−407.
69. Griffiths-Jonesa, S. R., Maynarda, A. J., and Searle, M. S. (1999) Dissecting the stability of a β-hairpin peptide that folds in water: NMR and molecular dynamics analysis of the β-turn and β-strand contributions to folding, *J. Mol. Biol. 292*, 1051−1069.
70. Sadqi, M., Lapidus, L. J., and Muñoz, V. (2003) How fast is protein hydrophobic collapse? *Proc. Natl. Acad. Sci. U.S.A. 100*, 12117−12122.

BI052039S